

Methane Exhaust Measurements at Gathering Compressor Stations in the United States

Timothy L. Vaughn,* Benjamin Luck, Laurie Williams, Anthony J. Marchese, and Daniel Zimmerle

Cite This: *Environ. Sci. Technol.* 2021, 55, 1190–1196

Read Online

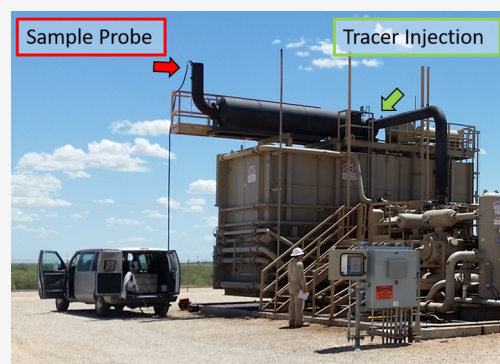
ACCESS |

Metrics & More

Article Recommendations

Supporting Information

ABSTRACT: Unburned methane entrained in exhaust from natural gas-fired compressor engines (“combustion slip”) can account for a substantial portion of station-level methane emissions. A novel in-stack, tracer gas method was coupled with Fourier transform infrared (FTIR) species measurements to quantify combustion slip from natural gas compressor engines at 67 gathering and boosting stations owned or managed by nine “study partner” operators in 11 U.S. states. The mean methane emission rate from 63 four-stroke, lean-burn (4SLB) compressor engines was 5.62 kg/h (95% CI = 5.15–6.17 kg/h) and ranged from 0.3 to 12.6 kg/h. The mean methane emission rate from 39 four-stroke, rich-burn (4SRB) compressor engines was 0.40 kg/h (95% CI = 0.37–0.42 kg/h) and ranged from 0.01 to 4.5 kg/h. Study results for 4SLB engines were lower than both the U.S. EPA compilation of air pollutant emission factors (AP-42) and Inventory of U.S. Greenhouse Gas Emissions and Sinks (GHGI) by 8 and 9%, respectively. Study results for 4SRB engines were 43% of the AP-42 emission factor and 8% of the GHGI emission factor, the latter of which does not distinguish between engine types. Total annual combustion slip from the U.S. natural gas gathering and boosting sector was modeled using measured emission rates and compressor unit counts from the U.S. EPA Greenhouse Gas Reporting Program. Modeled results [328 Gg/y (95% CI = 235–436 Gg/y) of unburned methane] would account for 24% (95% CI = 17–31%) of the 1391 Gg of methane emissions for “Gathering and Boosting Stations”, or 6% of the net emissions for “Natural Gas Systems” (5598 Gg) as reported in the 2020 U.S. EPA GHGI. Gathering and boosting combustion slip emissions reported in the 2020 GHGI (374 Gg) fall within the uncertainty of this model.



INTRODUCTION

U.S. natural gas production is expected to increase for the foreseeable future,¹ enhancing the need for reliable estimates of associated emissions. Accurately tracking emissions over time can help gauge whether the potential climate benefits associated with increased natural gas usage are being realized. Efforts to quantify emissions often disagree.^{2–8} Many speculate the disagreement may be due to spatio-temporal variability in emissions,^{9,10} or skewed emissions distributions where a small number of emitters accounts for a large portion of emissions (“super-emitters”).^{11,12} The stochastic nature of these phenomena presents a unique challenge for traditional inventory methods.

We have also seen that unburned methane entrained in exhaust from natural gas-fired compressor engines (“combustion slip”) can be a substantial source of methane emissions.¹³ Methods to estimate combustion slip emissions should be, comparatively, straightforward. Engine inventories are often reported or available, engines are often tested for compliance with state and federal regulations, and engines require tight control over process parameters for acceptable performance. The variance in emissions from engines providing acceptable performance is likely well-bounded relative to fugitive super-emitters. However, methane emissions are not often measured

during compliance tests because methane is not a regulated criteria pollutant. Never the less, several combustion slip emission factors are available and are commonly used, though their applicability to current natural gas gathering and boosting infrastructure is unclear.

In this study, combustion slip was measured in support of a larger effort to quantify total methane emissions from the U.S. natural gas gathering and boosting sector.¹⁴ Field measurements were made on 133 internal combustion engines used in gas compression service by nine U.S. gathering operators. Engines were selected randomly from those in service at 67 facilities in 11 U.S. states (see Figure S9). A novel, in-stack tracer gas method based on EPA Method ALT-012¹⁵ was used to quickly provide combustion slip estimates from engines operating as found, under normal daily circumstances. Combustion slip emission rates measured in the field were

Received: August 14, 2020
Revised: December 2, 2020
Accepted: December 3, 2020
Published: January 7, 2021



used in a Monte-Carlo model to estimate the total annual combustion slip from gas compression engines in use at U.S. natural gas gathering and boosting stations. Measured emission factors and model results were compared to the U.S. EPA compilation of air pollutant emission factors (AP-42), Inventory of U.S. Greenhouse Gas Emissions and Sinks (GHGI), and Greenhouse Gas Reporting Program: Subpart C (GHGRP). Suggestions for incorporating gathering and boosting combustion slip emissions into the GHGI are presented based on the results of this comparison.

METHODS

Study Design. Field measurements were made on 133 internal combustion engines used in gas compression service by nine U.S. gathering operators. Engines were selected randomly from those in service at 67 facilities in 11 U.S. states (see Figure S9) from July 30 to November 20, 2017. The in-stack tracer gas method (described below) was applied to units “as found” and therefore captured emissions during normal, day-to-day operations. Emissions during normal operations may differ from emissions observed during compliance tests, which require specific operating conditions. Additionally, concurrent exhaust stack flow measurements were made using both the in-stack tracer gas method and EPA Method 2¹⁶ on seven compressor engines during emission compliance tests administered by a third-party contractor. Results from each method were compared to better understand the performance of the in-stack tracer gas method under real-world conditions relative to an approved, established method.

Measurement Methods. The in-stack tracer method was used to collect in situ measurements of unburned methane entrained in the exhaust of natural gas compressor engines. This method involved injecting a tracer gas (CF₄) into the exhaust stream at a known flow rate and measuring concentrations of both the tracer gas and methane at the exit of the exhaust stack. The total exhaust flow was estimated from the tracer gas concentration measured at the exhaust stack exit using eq 1

$$\dot{Q}_{\text{exhaust}} = \frac{\dot{Q}_{\text{tracer}}}{C_{\text{tracer}}} \quad (1)$$

where \dot{Q} indicates tracer gas and exhaust stack volume flow rates in L/min and C indicates measured species concentrations in ppm-v. Equation 1 assumes that the injected tracer gas: (1) reached and remained in the exhaust stack; (2) was well mixed with the engine exhaust gases; and (3) did not react, dissociate, or adsorb in the exhaust stack; therefore, the tracer gas concentration measured at the exit was a result of dilution by the exhaust gas. In this study, tracer gas injection flow rates (0.05–0.5 SLPM) were negligible compared to total exhaust flow rates (20 000–200 000 SLPM). Tracer gas was undiluted prior to injection.

The flow rate of each species (e.g., CH₄) measured in the exhaust gas was estimated relative to the injected tracer gas flow rate as

$$\dot{Q}_{\text{CH}_4} = C_{\text{CH}_4} \frac{\dot{Q}_{\text{tracer}}}{C_{\text{tracer}}} \quad (2)$$

Since tracer gas injection was metered by mass flow controller, referenced to standard conditions, mass flow rates of pollutant species were calculated using their densities at the same standard conditions.

The in-stack tracer method is a direct extension of an EPA-approved alternative method “ALT-012: An Alternate Procedure For Stack Gas Volumetric Flow Rate Determination (Tracer Gas)”.¹⁵ The Alt-012 method recommends using sulfur hexafluoride (SF₆) as a tracer gas. SF₆ is “chemically inert, non-toxic, non-flammable, non-explosive and thermally stable (does not decompose in the gas phase below 500 °C)”,¹⁷ though others have noted decomposition to begin near 300 °C.¹⁸ Engine exhaust gas is typically at or above 500 °C, precluding the use of SF₆ as a tracer gas. In this study, carbon tetrafluoride (CF₄) was used as the tracer gas. Carbon tetrafluoride is: (1) a highly stable molecule that does not decompose below 1600 °C¹⁹ and (2) readily available from industrial suppliers as Refrigerant-14. Like SF₆, CF₄ is a strong infrared absorber and is easily measured by infrared spectroscopy at low concentrations.

During each test, pure CF₄ (R14 tetrafluoromethane 99.99%, Airgas, Inc.) was injected into the exhaust stack using a calibrated mass flow controller (MFC) (Alicat Scientific, MCM-5SLPM-D). The location of tracer gas injection varied depending on the configuration of the exhaust stack and availability of insertion ports (see Appendix A in ref 20). The engine exhaust gas (including tracer gas) was measured at the exit of the exhaust stack using Fourier-transform infrared spectroscopy (FTIR) (MKS, Multigas 2030). Exhaust gas was collected with a stainless steel sample probe and delivered to the FTIR using heated sample lines and a heated-head sample pump operating at 191 °C. If the stack diameter was ≥6 in., a multiport sample probe with holes at 16.7, 50, and 83.3% of the diameter was used. If the stack diameter was <6 in., a single-point probe was used. The quality assurance procedures used to ensure properly delivered, well-mixed tracer gas, and accurate FTIR measurements within the exhaust stack are described in Section S1.1.

Analysis Methods. Time series data from the tracer gas MFC and the FTIR were recorded at 0.1 Hz. Time series data from each test were reduced to mean values and an associated uncertainty term. Mean values and associated uncertainties from each test on a single unit were then combined to produce an overall combustion slip estimate (with uncertainty) for that unit.

Tracer gas flow rate data from a single test were reduced from a time series to a mean value with uncertainty using the logic shown in ref 20—Figure S2-2. First, the arithmetic mean and the standard deviation of the time series data were computed. Next, the uncertainty was estimated using two methods: (1) by multiplying the MFC manufacturer-specified instrument error (in percent) by the arithmetic mean and (2) by calculating the standard deviation of the time series data. The greater of these two uncertainty values was considered the uncertainty for the test. When the physical test setup enabled a steady tracer gas flow rate with little variation about the set point, it was appropriate to use the instrument uncertainty. When the physical test setup caused flow variations about the set point in excess of the instrument uncertainty, the uncertainty was estimated more conservatively using the standard deviation of the time series.

Reducing methane and tracer gas concentration measurements from the FTIR required a more complicated approach to account for measurement interference from excessive water vapor present in exhaust streams (see Section S1.2 and ref 20—Figure S2-3). During some tests, high water vapor concentrations caused intermittent water vapor spikes that

Table 1. Study-Measured and EPA Emission Factor Comparison^a

	engines			IGT	units	basis
	2SLB	4SLB	4SRB			
study		1.15	0.10		lb/MMBtu	fuel input
AP 42	1.45	1.25	0.23	0.0086	lb/MMBtu	fuel input
GHGI ^b	1.27	1.27	1.27	0.0044	lb/MMBtu	fuel input
GHGRP	0.002	0.002	0.002	0.002	lb/MMBtu	fuel input

^aThe emission factors represent the quantity of unburned fuel emitted as CH₄ on a lb CH₄/MMBtu fuel input basis. ^bBased on underlying emission tests to exclude the effects of activity weighting, converted assuming 19.2 g/scf CH₄ ≈ 19.2 g/scf fuel, 1026 Btu/scf fuel, for comparison (see eq 5).

attenuated measurements of other species. An example is shown in ref 20—Figure S2-4, where one can see that measurements of the tracer gas (CF₄) are inversely correlated with H₂O measurements. These spikes were attributed to condensation and subsequent re-vaporization of water vapor within the FTIR sample train. Insulating unheated fittings in the FTIR sample train helped reduce water spikes but did not eliminate them. Active heating of exposed fittings may be required to eliminate cold spots during tests of engines fueled by wet, high-Btu field gas.

Methane emission rates for each test on each unit were calculated by multiplying stack flow rates by methane concentrations measured by FTIR (including uncertainty terms). When multiple tests were performed on a unit, overall emission rates for the unit were computed using a weighted mean

$$\bar{x}_w = \frac{\sum w_i x_i}{\sum w_i} \quad (3)$$

where x_i is the emission rate of each test, weighted by w_i , the number of samples in test i . The uncertainty terms for each test on a unit were reduced to a single value using a pooled, relative uncertainty:-

$$s_{r,p} = \sqrt{\frac{\sum (w_i - 1) s_{r,i}^2}{\sum w_i - 1}} \quad (4)$$

where w_i is the number of samples in test i , and $s_{r,i}$ is the relative uncertainty for test i .

Comparison to EPA Emission Factors. Study-estimated combustion slip was compared to estimates developed using emission factors from AP-42,²¹ the GHGI,²² and the GHGRP.²³ Results were normalized to AP-42 basis, units, and type-classifications for the comparison. AP-42 emission factors are provided in units of lb/MMBtu on the basis of fuel input. The AP-42 compilation lists combustion slip emission factors for four types of internal combustion-powered compressor drivers: two-stroke, lean-burn (2SLB); four-stroke, lean-burn (4SLB); four-stroke, rich-burn (4SRB); and industrial gas turbines (IGT). These categories encompass all commonly used compressor engine drivers except electric-powered motors. Prior to 2020, the GHGI used facility-scale emission factors for gathering and boosting. However, combustion slip emission factors were used for gas compression prime-movers in service at transmission and storage, and processing plants; one for reciprocating compressor engines (2SLB, 4SLB, 4SRB; inclusive), and one for turbines (IGT) (“GHGI”, as used herein). The GHGRP uses one combustion slip emission factor for all internal combustion compressor drivers. In the current study, emission

factors were developed from field measurements of 4SLB and 4SRB compressor driver engines. Based on compressor driver data from study partners, these two engine types encompass most engines used in gas compression applications in the gathering and boosting sector, though 2SLB, IGT and electric motor drivers are sometimes used. Unit types and counts by basin as reported by study partners are shown in Table S2.

An estimate of fuel consumption was needed to calculate comparable emissions. Engine manufacturer data indicated that brake specific fuel consumption (BSFC) generally increased as engine load decreased. Sample BSFC curves from manufacturer data for four engine models frequently encountered during the field campaign (two 4SRB models, two 4SLB models) were used to generate a model BSFC versus load curve that was used to estimate fuel consumption for all engines (see ref 20—Figure S2-15). Operating loads observed during testing were applied directly to the engines they were observed on (see ref 20—Figure S2-14). For engines where loads were not available during testing, average loads specific to each unit type (4SRB, 4SLB) were assigned. Modeled BSFC and operating loads were then used to estimate combustion slip (see Table 1) on the basis of fuel energy input.

The combustion slip emission factors used in the GHGI (0.24 scf CH₄/hp-h for engines, 0.0057 scf CH₄/hp-h for turbines) originate from a 1996 GRI/EPA report²⁴ and include activity weighting. Tables 1 and S1 show average GHGI emission factors developed from the underlying test data (0.0307 lb CH₄/lb fuel input for engines, and 0.000107 lb of CH₄/lb fuel input for turbines), which exclude activity weighting and are therefore directly comparable to AP-42 and study emission factors. To normalize emission rates underlying the GHGI to AP-42 units and basis, the following equation was used

$$\begin{aligned} \text{GHGI} &= 0.0307 \frac{\text{lb CH}_4}{\text{lb fuel}} \cdot \frac{19.2 \text{ lb fuel}}{453.6 \text{ scf fuel}} \cdot \frac{1 \text{ scf fuel}}{1026 \text{ Btu fuel}} \\ &= 1.27 \frac{\text{lb CH}_4}{\text{MMBtu fuel}} \end{aligned} \quad (5)$$

where it is assumed that the density of fuel is approximately equal to methane (19.2 g/scf CH₄ ≈ 19.2 g/scf fuel, 453.6 g/lb is a conversion factor), and that 1 scf of fuel contains 1026 Btu, for comparison. The result is expressed in lbs of methane emitted per million Btu of fuel input to the engine, the same basis as the AP-42 factors. An analogous approach was used to convert the GHGI turbine emission factor. GHGRP emissions were calculated using the Subpart C combustion slip emission factor (0.001 kg CH₄/MMBtu fuel input).

National Combustion Slip Estimates. National estimates of combustion slip emissions from gathering and boosting compressor engines were developed by applying

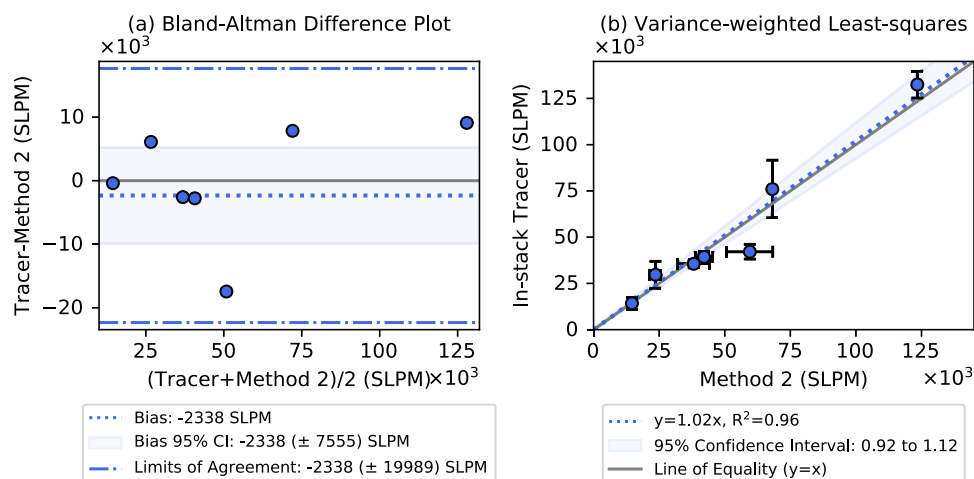


Figure 1. Compressor engine exhaust stack flows predicted by the in-stack tracer method agree with concurrent EPA Method 2 estimates when compared by (a) Bland–Altman difference plot and (b) variance-weighted, least-squares regression.

study, AP-42, GHGI, and GHGRP emission factors to compressor engines operated by study partners and then by scaling up by compressor counts reported to the U.S. EPA GHGRP in a Monte-Carlo model. Study partners operate 4794 compressor units at 1700 facilities in 28 American Association of Petroleum Geologists basins (provinces),²⁵ or 30% of the units reported to the 2017 GHGRP. Unit counts by basin and unit type are shown in Table S2. For the study estimate, subcategories were added to AP-42, 4SLB, and 4SRB type-classifications for units frequently encountered during the field campaign. Two subcategories were added for 4SLB units (G3500 and G3600; see Figure S2), and one was added for 4SRB units (VHP_4SRB).

Study partners provided lists of compressor units by facility. Provided data varied in specificity from number of units only, to complete descriptions including make, model, AP-42 type, and rated horsepower. Data for units with partial descriptions were inferred from other units in the lists, manufacturer data sheets, state air permits/applications, and previous reports on emissions from compressor engines.^{26,27} The resulting unit list used to develop the national combustion slip estimate is included in the Supporting Data file “CompressorDriverUnitList.csv”. Ninety-three percent of units were fully categorized for emissions modeling using provided data. Remaining units were modeled by re-sampling from categorized units considering available descriptors. For example, units with no identifying characteristics were simulated by re-sampling from all possible units (including electrically driven compressors); units of known AP-42 type were re-sampled from categorized units of the same type.

A total of 5000 combustion slip estimates were calculated for each of 4794 study partner compressor units using study and EPA emission factors. Calculations considered the distribution of operating loads observed during the field study (see Figure S4). Simulated engines were then grouped by facility, and set to “operating” or “not operating” based on utilization observed during the field study. In this way, emissions from some units were set to zero so that the national estimate represents emissions from the portion of the national fleet operating at any one time.

Basins with 20 or more study partner units were simulated by re-sampling from combustion slip estimates of units within that basin. Basins with fewer than 20 units were simulated by

re-sampling from all study partner units. Each basin was simulated by drawing an appropriate number of units from basin unit counts in the 2017 GHGRP. Unit counts in each basin were modified by an estimated fraction of screw compressors, as only reciprocating and centrifugal units are reported to the GHGRP. Emissions were summed across all basins to yield national estimates.

RESULTS AND DISCUSSION

Exhaust Stack Flow Rates. Exhaust stack flows predicted by the in-stack tracer method agreed with those obtained using EPA Method 2 when compared using Bland–Altman difference plots and variance-weighted, least-squares regression (VWLS). In Figure 1a, the difference of in-stack tracer and EPA Method 2 is plotted against the mean of in-stack tracer and EPA Method 2. The “bias” (mean of differences, dotted line) is negative, indicating that in-stack tracer may predict lower flow rates than EPA Method 2. However, a 95% confidence interval on the bias (shaded area) includes $y = 0$, which indicates that the bias is not significant at the 95% confidence level for this dataset. In Figure 1b, paired measurements are compared using VWLS, which considers the uncertainty in both measurements at each data point. The slope of the VWLS regression is 1.02 and the 95% confidence interval about the VWLS regression slope includes the line of equality ($y = x$), indicating that the methods agree at the 95% confidence level.

Stack flows predicted by the in-stack tracer method were also compared to manufacturer exhaust flow specifications (see ref 20—Section S2-4) for 42 units where operational data needed to estimate stack flows were available. The qualitative agreement between the in-stack tracer method and manufacturer-specified exhaust stack flow rates is shown in ref 20—Figure S2-12 for both 4SRB (ordinary least-squares regression ($1.19x - 8.99e3$, $R^2 = 0.95$)) and 4SLB (ordinary least-squares regression ($0.89x + 8.92e3$, $R^2 = 0.95$)) gas compressor engines.

In-stack methane concentrations were measured using FTIR spectroscopy and combined with exhaust stack flow rates to estimate combustion slip. FTIR measurements of calibration gases indicate accurate methane concentration measurements (see ref 20—Section S2-2.3). Since total stack flow estimates agreed with independent EPA Method 2 estimates (and

manufacturer specifications) and measured species concentrations agreed with reference gas concentrations, we expect that combustion slip emission rates were estimated with reasonable accuracy by eq 2. This expectation is supported by comparison with secondary estimates made using EPA Method 19²⁸ for measured units where gas property data needed to calculate *F*-factors were available (ordinary least-squares regression ($1.00x + 2.2e-3$, $R^2 = 0.96$); see ref 20—Figure S2-16).

Comparison to EPA Emission Factors. Study-measured and EPA emission factors are compared in Table 1. As others have noted previously, the methane combustion slip factor used in the GHGRP (subpart C) does not accurately characterize combustion slip from any class of internal combustion device and is likely underestimating emissions from IGTs by a factor of 2–4, and from engines by 3 orders of magnitude. Relative to AP-42, the measured emission rates underlying the GHGI (activity-weighted) emission factors predict half the combustion slip for IGTs, compare well for 2SLBs (12% lower) and 4SLBs (2% higher), and overestimate for 4SRBs (factor of 5 higher). Without access to the original test database, it may be that 4SRB engines were not represented proportionally across the three engine types in the underlying data.

Study emission factors compare well with AP-42 for 4SLBs (9% lower), but underestimate combustion slip emissions for 4SRBs by a factor of two. One possible explanation is that the AP-42 factors were based on tests of units that did not employ exhaust after treatment. During the study, all 4SRB engines tested were equipped with nonselective catalytic reduction (NSCR) after treatment, which may help explain the reduction in combustion slip relative to the AP-42 factor. The results in Table 1 are also shown on the basis of % of fuel input in Table S1. The test data underlying study emission factors are shown in Figures S1–S3.

Average, per unit emissions for each of the engine types were also computed as shown in Table 2. In Table 2, study results

Table 2. Summary Table of Average Combustion Slip Per Unit (kg CH₄/h/Unit) Evaluated with Each Emission Factor across Tested Units

	4SRB	4SLB
	avg. (kg/h/unit)	avg. (kg/h/unit)
study-measured	0.40 (0.24–0.68)	5.77 (5.03–6.50)
study EF	0.40 (0.37–0.42)	5.62 (5.15–6.17)
AP-42	0.94 (0.87–1.00)	6.13 (5.63–6.73)
GHGI	5.09 (4.72–5.41)	7.20 (6.55–7.97)
GHGRP	0.01 (0.01–0.01)	0.01 (0.01–0.01)

are shown as measured values, and then as study emission factors developed from the measured values. Study emission factors were applied to the sample population in the same way as the EPA emission factors. In this comparison, the GHGI emission factor (0.24 scf CH₄/hp-h) was applied directly, not the average emission rate from underlying test data as in ref 20—Section S2-5.1.

The average emission rates for units measured in the field campaign (study emission factors) were found to be 0.40 kg/h (−0.03/+0.02) kg/h/unit for 4SRB units, and 5.62 (−0.47/+0.55) kg/h/unit for 4SLB units, based on study emission factors, as shown in ref 20—Figure S2-20. When applied to the count of study-measured engines in each classification, total

emissions are 16 (14–16) kg/h for 4SRB units and 354 (325–389) kg/h for 4SLB units. Total emissions and average emissions per unit were calculated in a similar manner for AP-42, GHGI, and GHGRP emission factors in ref 20—Figures S2-21, S2-22, and S2-23, respectively, and are compared in Table 2.

The confidence intervals derived based on directly measured values are large relative to those derived from the emission factors because they include the full range of emission rates measured, and not the more limited range that would result from using an average emission factor. For this reason, study emission factors were developed from the measured values and compared to the EPA emission factors. Note the similar shape of each distribution in ref 20—Figures S2-21, S2-22, S2-23, and the study emission factors in ref 20—Figure S2-20. The consistent distribution shapes in these figures illustrate that results are compared on the same basis. Emission rate differences are due only to scaling by the emission factor and not other underlying assumptions. As shown in Table 2, calculated CH₄ emissions per unit for 4SRB units show more variability than 4SLB units, and none of the confidence intervals overlap. Similar to the discussion above, AP-42 estimates twice the emissions as the study EF for 4SRB units, while the GHGI greatly overestimates and GHGRP greatly underestimates emissions. For 4SLB units, AP-42 estimates greater emissions than the study EF; however, the 95% confidence intervals overlap, indicating that for the population of units tested, the AP-42 4SLB factor would have adequately estimated combustion slip emissions for this unit type, in this study. The GHGI emission factor also overestimates combustion slip emissions relative to the 4SLB study EF, and the confidence intervals do not overlap. The GHGRP factor grossly underestimates emissions from both engine types.

National Combustion Slip Estimate. National combustion slip estimates were made using study, AP-42, GHGI, and GHGRP emission factors; results are shown in Table 3. Study-

Table 3. National Combustion Slip Emissions from Gathering Compressor Units Estimated by Study, AP-42, GHGI, and GHGRP Emission Factors^a

estimate	kg/h	kg/h CI	Gg/y	Gg/y CI
study	37 437	(26 870–49 746)	328	(235–436)
AP-42	49 367	(34 919–65 711)	432	(306–576)
GHGI	72 779	(50 990–97 059)	638	(447–850)
SubC	125	(88–166)	1	(1–1)

^aGathering combustion slip emission reported in the 2020 GHGI³¹ (374 Gg) fall within the uncertainty range of the study and AP-42 model estimates.

modeled combustion slip emissions are also shown by production basin in Table S3 and Figure S10. Estimates made using AP-42 and GHGI emission factors predicted higher emissions than study factors while the GHGRP Subpart C estimate underpredicted emissions substantially. AP-42 predicted 32% greater emissions, and GHGI predicted 94% greater emissions than study results. However, 95% confidence intervals for national estimates overlapped among study and AP-42 estimates. This may not always be the case when considering subsets of units at the basin or facility level. For subsets with mostly 4SLB units, predicted results should be similar given the similar emission factors. AP-42 and GHGI

emission factors would increasingly over-predict emissions relative to the study as the fraction of 4SRB engines in a subset increased. It should be noted that none of these estimates include unburned methane emissions from crankcase ventilation systems which were not a focus of this study. For example, crankcase ventilation systems on 4SLB engines may add another 3–20% to each estimate.^{29,30}

The study-estimated national combustion slip emission rate was 37 437 kg/h (95% CI = 26 870–49 746 kg/h) or 328 Gg/y (95% CI = 235–436 Gg/y), which represents 24% (95% CI = 17–31%) of the 1391 Gg of methane emissions from “Gathering and Boosting Stations” reported in the 2020 U.S. EPA GHGI.³¹ The study estimate is 12% lower than that reported in the 2020 GHGI³¹ (374 Gg), which was derived from an early summary of this work in Zimmerle et al.,¹⁴ as described in the 2020 GHGI Gathering and Boosting update.³¹ Slightly different model assumptions on compressor counts, operating loads, and utilization rates lead to this difference, which falls well within stated model uncertainties.

It is clear from study results that the GHGRP combustion slip emission factor is inadequate for internal combustion engines and should not be used in the GHGI. The GHGI emission factor may better represent emissions from engines in the transmission, storage, and processing sectors due to the types of engines tested in the underlying data. AP-42 CH₄ combustion slip emission factors compared best with study results, though several differences were observed. First, the emission factor developed from 4SRB engines observed during the study was 43% of the current AP-42 factor. This may be due to the presence of exhaust after treatment on all 4SRB units observed in the study, whereas the current AP-42 factor is for uncontrolled engines. Second, the study revealed very different emissions from two subtypes of engines that would both fall under the AP-42 4SLB classification (see Figure S2). The reason for this is not fully understood, though the use of pre-chambers for ultra-lean combustion appears to be a distinguishing characteristic.

A model was formulated that demonstrated a method to estimate national gathering and boosting combustion slip emissions, by basin, utilizing compressor activity data from the GHGRP (see Figure S9). The model considered the mix of driver types currently installed, by basin, based on study partner-provided data (see Table S2). Observed engine types, operating loads, and utilization rates (i.e., units running at visited stations) were considered in the model. The model used recent, direct measurements of combustion slip emissions from 133 compressor units and should therefore more accurately reflect current emissions compared to cataloged emission factors. Combining study emission factors (including subcategories) with activity data similar to those in Table S2 would provide an accurate method for future combustion slip estimates from gathering and boosting.

■ ASSOCIATED CONTENT

SI Supporting Information

The Supporting Information is available free of charge at <https://pubs.acs.org/doi/10.1021/acs.est.0c05492>.

Modeled engines with counts: <https://pubs.acs.org/doi/10.1021/acs.est.0c05492>. Ref 20- Appendix A: Stack testing data summary (16.49Mb), <http://dx.doi.org/10.25675/10217/194540>. Ref 20- Data_Volume2.zip (15.58Kb), <http://dx.doi.org/10.25675/10217/194766>.

Study archive: <https://mountainscholar.org/handle/10217/195489> (TXT)

Study-measured and EPA emission factor comparison; test data underlying study emission factors; percent load, as noted during testing on engines equipped with control panel displays; fraction of BSFC vs fraction of rated load; field measurements; tracer gas injections rates; test locations by state and EIA basin; combustion slip estimate by basin for basins reporting to the 2017 US EPA GHGRP; study partner compressor unit types by basin; and combustion slip estimate by basin (PDF)

■ AUTHOR INFORMATION

Corresponding Author

Timothy L. Vaughn – Energy Institute, Colorado State University, Fort Collins, Colorado 80524, United States; orcid.org/0000-0001-7375-2594; Email: tim.vaughn@colostate.edu

Authors

Benjamin Luck – Energy Institute, Colorado State University, Fort Collins, Colorado 80524, United States

Laurie Williams – Fort Lewis College, Durango, Colorado 81301, United States

Anthony J. Marchese – Energy Institute, Colorado State University, Fort Collins, Colorado 80524, United States; Mechanical Engineering, Colorado State University, Fort Collins, Colorado 80523, United States

Daniel Zimmerle – Energy Institute, Colorado State University, Fort Collins, Colorado 80524, United States; orcid.org/0000-0003-2832-048X

Complete contact information is available at: <https://pubs.acs.org/10.1021/acs.est.0c05492>

Notes

The authors declare no competing financial interest.

■ ACKNOWLEDGMENTS

Funding for this work was provided by the National Energy Technology Laboratory, Office of Fossil Energy Contract DE-FE0029068 awarded to Colorado State University. Cost share for this project was provided by Anadarko Petroleum Corporation, the Colorado Energy Research Collaboratory, the Colorado Energy Office, DCP Midstream, Kinder Morgan Natural Gas Pipelines, Mark West Energy Partners, ONE Future, Pioneer Natural Resources, Southwestern Energy, Equinor (formerly Statoil Gulf Services), Williams, and XTO Energy, Inc. Industry operators provided operational data and/or site access as well as detection and measurement support in many cases. Additional data were also provided by GSI Environmental (through DOE Contract DE-FE0029084). The authors greatly appreciate the significant, coordinated efforts of all field measurement personnel and those who aided in data compilation.

■ REFERENCES

- (1) EIA. Annual Energy Outlook. 2019. <https://www.eia.gov/outlooks/aeo/>.
- (2) Brandt, A. R.; Heath, G. A.; Kort, E. A.; O'Sullivan, F.; Pétron, G.; Jordaan, S. M.; Tans, P.; Wilcox, J.; Gopstein, A. M.; Arent, D.; Wofsy, S.; Brown, N. J.; Bradley, R.; Stucky, G. D.; Eardley, D.; Harriss, R. Methane Leaks from North American Natural Gas Systems. *Science* **2014**, *343*, 733–735.

- (3) Alvarez, R. A.; Zavala-Araiza, D.; Lyon, D. R.; Allen, D. T.; Barkley, Z. R.; Brandt, A. R.; Davis, K. J.; Herndon, S. C.; Jacob, D. J.; Karion, A.; Kort, E. A.; Lamb, B. K.; Lauvaux, T.; Maasakkers, J. D.; Marchese, A. J.; Omara, M.; Pacala, S. W.; Peischl, J.; Robinson, A. L.; Shepson, P. B.; Sweeney, C.; Townsend-Small, A.; Wofsy, S. C.; Hamburg, S. P. Assessment of Methane Emissions from the U.S. Oil and Gas Supply Chain. *Science* **2018**, *361*, 186–188.
- (4) Peischl, J.; Karion, A.; Sweeney, C.; Kort, E. A.; Smith, M. L.; Brandt, A. R.; Yeskoo, T.; Aikin, K. C.; Conley, S. A.; Gvakharia, A.; Trainer, M.; Wolter, S.; Ryerson, T. B. Quantifying Atmospheric Methane Emissions from Oil and Natural Gas Production in the Bakken Shale Region of North Dakota. *J. Geophys. Res.* **2016**, *121*, 6101–6111.
- (5) Karion, A.; Sweeney, C.; Pétron, G.; Frost, G.; Michael Hardesty, R.; Kofler, J.; Miller, B. R.; Newberger, T.; Wolter, S.; Banta, R.; Brewer, A.; Dlugokencky, E.; Lang, P.; Montzka, S. A.; Schnell, R.; Tans, P.; Trainer, M.; Zamora, R.; Conley, S. Methane Emissions Estimate from Airborne Measurements over a Western United States Natural Gas Field. *Geophys. Res. Lett.* **2013**, *40*, 4393–4397.
- (6) Pétron, G.; Karion, A.; Sweeney, C.; Miller, B. R.; Montzka, S. A.; Frost, G. J.; Trainer, M.; Tans, P.; Andrews, A.; Kofler, J.; Helmig, D.; Guenther, D.; Dlugokencky, E.; Lang, P.; Newberger, T.; Wolter, S.; Hall, B.; Novelli, P.; Brewer, A.; Conley, S.; Hardesty, M.; Banta, R.; White, A.; Noone, D.; Wolfe, D.; Schnell, R. A New Look at Methane and Nonmethane Hydrocarbon Emissions from Oil and Natural Gas Operations in the Colorado Denver-Julesburg Basin. *J. Geophys. Res.* **2014**, *119*, 6836–6852.
- (7) Caulton, D. R.; Lu, J. M.; Lane, H. M.; Buchholz, B.; Fitts, J. P.; Golston, L. M.; Guo, X.; Li, Q.; McSpirt, J.; Pan, D.; Wendt, L.; Bou-Zeid, E.; Zondlo, M. A. Importance of Superemitter Natural Gas Well Pads in the Marcellus Shale. *Environ. Sci. Technol.* **2019**, *53*, 4747–4754.
- (8) Duren, R. M.; Thorpe, A. K.; Foster, K. T.; Rafiq, T.; Hopkins, F. M.; Yadav, V.; Bue, B. D.; Thompson, D. R.; Conley, S.; Colombi, N. K.; Frankenberg, C.; McCubbin, I. B.; Eastwood, M. L.; Falk, M.; Herner, J. D.; Croes, B. E.; Green, R. O.; Miller, C. E. Californiaas Methane Super-Emitters. *Nature* **2019**, *575*, 180–184.
- (9) Lavoie, T. N.; Shepson, P. B.; Cambaliza, M. O. L.; Stirn, B. H.; Conley, S.; Mehrotra, S.; Faloon, I. C.; Lyon, D. Spatiotemporal Variability of Methane Emissions at Oil and Natural Gas Operations in the Eagle Ford Basin. *Environ. Sci. Technol.* **2017**, *51*, 8001–8009.
- (10) Vaughn, T. L.; Bell, C. S.; Pickering, C. K.; Schwietzke, S.; Heath, G. A.; Pétron, G.; Zimmerle, D. J.; Schnell, R. C.; Nummedal, D. Temporal Variability Largely Explains Top-down/Bottom-up Difference in Methane Emission Estimates from a Natural Gas Production Region. *Proc. Natl. Acad. Sci. U.S.A.* **2018**, *115*, 11712–11717.
- (11) Lyon, D. R.; Zavala-Araiza, D.; Alvarez, R. A.; Harriss, R.; Palacios, V.; Lan, X.; Talbot, R.; Lavoie, T.; Shepson, P.; Yacovitch, T. I.; Herndon, S. C.; Marchese, A. J.; Zimmerle, D.; Robinson, A. L.; Hamburg, S. P. Constructing a Spatially Resolved Methane Emission Inventory for the Barnett Shale Region. *Environ. Sci. Technol.* **2015**, *49*, 8147–8157.
- (12) Zavala-Araiza, D.; Lyon, D.; Alvarez, R. A.; Palacios, V.; Harriss, R.; Lan, X.; Talbot, R.; Hamburg, S. P. Toward a Functional Definition of Methane Super-Emitters: Application to Natural Gas Production Sites. *Environ. Sci. Technol.* **2015**, *49*, 8167–8174.
- (13) Vaughn, T. L.; Bell, C. S.; Yacovitch, T. I.; Roscioli, J. R.; Herndon, S. C.; Conley, S.; Schwietzke, S.; Heath, G. A.; Pétron, G.; Zimmerle, D. Comparing Facility-Level Methane Emission Rate Estimates at Natural Gas Gathering and Boosting Stations. *Elementa: Sci. Anthropocene* **2017**, *5*, No. 71.
- (14) Zimmerle, D.; Vaughn, T.; Luck, B.; Lauderdale, T.; Keen, K.; Harrison, M.; Marchese, A.; Williams, L.; Allen, D. Methane Emissions from Gathering Compressor Stations in the U.S. *Environ. Sci. Technol.* **2020**, *54*, 7552–7561.
- (15) US EPA OAR. Broadly Applicable Approved Alternative Test Methods. <https://www.epa.gov/emc/broadly-applicable-approved-alternative-test-methods>.
- (16) US EPA. Method 2—Velocity-S-Type Pitot. <https://www.epa.gov/emc/method-2-velocity-s-type-pitot>.
- (17) Christophorou, L. G.; Olthoff, J. K.; Brunt, R. J. V. Sulfur Hexafluoride and the Electric Power Industry. *IEEE Electr. Insul. Mag.* **1997**, *13*, 20–24.
- (18) Pan, J.; Tang, J.; Yao, Q.; Wang, C.; Zeng, F. In *Study on SF6 Decomposition Characteristics under Thermal Fault and Its Representation Method*. 2013 Annual Report Conference on Electrical Insulation and Dielectric Phenomena, 2013; pp 73–76.
- (19) Qin, L.; Han, J.; Wang, G.; Kim, H. J.; Kawaguchi, I. Highly Efficient Decomposition of CF₄ Gases by Combustion. *Sci. Res.* **2010**, 126–130.
- (20) Vaughn, T.; Luck, B.; Zimmerle, D.; Marchese, A.; Williams, L.; Keen, K.; Lauderdale, T.; Harrison, M.; Allen, D. *Methane Emissions from Gathering and Boosting Compressor Stations in the U.S. Supporting Volume 2: Compressor Engine Exhaust Measurements*; 2019.
- (21) US EPA. AP-42 Section 3.2 Natural Gas-Fired Reciprocating Engines. <http://www.epa.gov/ttn/chief/ap42/ch03/related/c03s02.html>.
- (22) US EPA. *Inventory of U.S. Greenhouse Gas Emissions and Sinks: 1990–2016, Annex 3*; 2018.
- (23) 40 C.F.R. § 98.33, Mandatory Greenhouse Gas Reporting Subpart C: General Stationary Fuel Combustion Sources.
- (24) Stapper, C. J. *Methane Emissions from the Natural Gas Industry, Volume 11: Compressor Driver Exhaust; Reports and Assessments*; 2016.
- (25) National Geologic Map Database. <https://ngmdb.usgs.gov/Geolex/strates/provinces>.
- (26) Pring, M.; Hudson, D.; Renzaglia, J.; Smith, B.; Treimel, S. *Characterization of Oil and Gas Production Equipment and Develop a Methodology to Estimate Statewide Emissions*; 2010.
- (27) Hohn, K.; Nuss-Warren, S. R. *Cost-Effective Reciprocating Engine Emissions Control and Monitoring for E&P Field and Gathering Engines*; 2011.
- (28) US EPA. Method 19—Sulfur Dioxide Removal and Particulate, Sulfur Dioxide and Nitrogen Oxides from Electric Utility Steam Generators. <https://www.epa.gov/emc/method-19-sulfur-dioxide-removal-and-particulate-sulfur-dioxide-and-nitrogen-oxides-electric>.
- (29) Caterpillar. Caterpillar Application & Installation Guide Crankcase Ventilation Systems. [s7d2.scene7.com/is/content/Caterpillar/CM20160713-53120-62603](https://www.caterpillar.com/content/Caterpillar/CM20160713-53120-62603).
- (30) Johnson, D. R.; Covington, A. N.; Clark, N. N. Methane Emissions from Leak and Loss Audits of Natural Gas Compressor Stations and Storage Facilities. *Environ. Sci. Technol.* **2015**, *49*, 8132–8138.
- (31) US EPA. Natural Gas and Petroleum Systems in the GHG Inventory: Additional Information on the 1990–2018 GHG Inventory. 2020. <https://www.epa.gov/ghgemissions/natural-gas-and-petroleum-systems-ghg-inventory-additional-information-1990-2018-ghg>.